Shot noise in coupled electron-boson systems

Yiming Wang,[1] Shouvik Sur,[1] Chandan Setty,[1] and Qimiao Si[1]

[1] *Department of Physics and Astronomy, Rice Center for Quantum Materials, Rice University, Houston, Texas 77005, USA*

The nature of charge carriers in strange metals has become a topic of intense current investigation. Recent shot noise measurements in the quantum critical heavy fermion metal $YbRh_2Si_2$ revealed a suppression of the Fano factor that cannot be understood from electron-phonon scattering or strong electron correlations in a Fermi liquid, indicating loss of quasiparticles. The experiment motivates the consideration of shot noise in a variety of theoretical models in which quasiparticles may be lost. Here we study shot noise in systems with co-existing itinerant electrons and dispersive bosons, going beyond the regime where the bosons are on their own in thermal equilibrium. We construct the Boltzmann-Langevin equations for the coupled system, and show that adequate electron-boson couplings restore the Fano factor to its Fermi liquid value. Our findings point to the beyond-Landau form of quantum criticality as underlying the suppressed shot noise of strange metals in heavy fermion metals and beyond.

Introduction: In conventional metals described by Landau Fermi liquid theory, the scattering rate increases quadratically with temperature, and the electrical current is carried by well-defined quasiparticles with electronic charge e [1]. However, in strange metals, like quantum critical heavy fermion materials [2], resistivity increases linearly with temperature, and quasiparticles may lose their identity [3, 4]. This requires a new description beyond the Landau paradigm, which may no longer involve discrete current carriers. Shot noise provides a non-equilibrium probe of the granularity of charge carriers [5, 6], helping to clarify the nature of current carriers in these enigmatic metals.

The shot noise Fano factor (F) measures the low-frequency current fluctuations relative to the average current, serving as a valuable indicator of discreteness of the current carriers. Recent measurements in the quantum critical heavy fermion metal $YbRh_2Si_2$ revealed a strong suppression of the Fano factor in the strange metal regime [7], which cannot be attributed to electron-phonon interactions in a Fermi liquid. The experiment has motivated theoretical studies of shot noise in strongly correlated metals [8–10]. In particular, we found that when the current is carried by quasiparticles, the Fano factor $F = \sqrt{3}/4$ even when the renormalization effect is extremely strong as in heavy Fermi liquids [8]. This implies that quasiparticles *must* be destroyed to account for the shot-noise reduction, a conclusion that is consistent with the beyond-Landau form of quantum criticality advanced for heavy fermion metals [11–13]; it also is supported by the overall phenomenology of $YbRh_2Si_2$ and related quantum critical heavy fermion metals [14, 15], which includes Fermi surface jump across the quantum critical point (QCP) [16–18] and dynamical Planckian scaling at the QCP [19–21]. This conclusion also implies that the Fano factor joins the Weidemann-Franz law [22, 23] and Kadowaki-Woods ratio [24, 25] as a valuable tool for characterizing strong correlations in diffusive Fermi liquids and diagnosing quasiparticle loss.

To further sharpen the considerations, here we study shot noise in coupled electron-boson systems. We take cue from the known result about the effect of electron-phonon scattering when the phonons are in equilibrium on their own as illustrated in Fig. 1(a): when this scattering is operative, which happens when the corresponding scattering length l_{eb} falls below the system size L, the

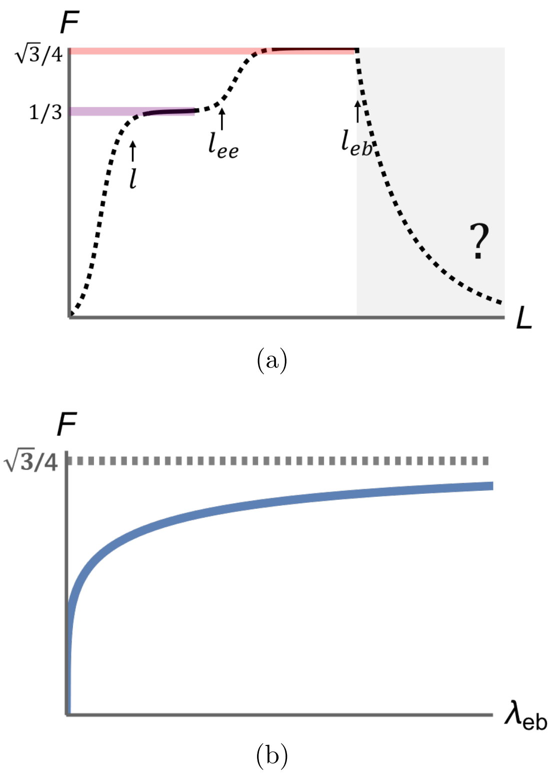

FIG. 1. (a) Schematic plot of the Fano factor (F) as a function of system size L, initially derived based on a Fermi gas experiencing electron-electron and electron-phonon scattering [26–29]. With the phonons taken as in equilibrium on its own, the electron-phonon coupling equilibrates the electron distribution and, thus, reduces the Fano factor, when the system size L exceeds the scattering lengths l_{eb}. Here we ask what happens if the bosons are not assumed to be in equilibrium. (b) Schematic result for the Fano factor as a function of the electron-boson coupling, λ_{eb}, when the bosons are allowed to be out of equilibrium.

electron-phonon coupling equilibrates the electron distribution and, thus, reduces the Fano factor [26–29]. While this phonon-based mechanism per se was ruled out for $YbRh_2Si_2$ through measurements of long wires [7], it provides a concrete setting for addressing the following question: What happens to the shot noise in coupled electron-boson systems when the bosons can be driven out of equilibrium through their coupling with the electrons? This question is relevant for the electron-boson problem in the boson-drag regime, where the momentum or energy transferred from the electrons to the boson component can be transferred back to the electron component. While the drag effect for the electron-phonon problem is negligible except for extreme low temperatures, it is expected to be important for the cases where the bosons are collective modes of the electron system due to a large electron-boson coupling (which traces back to the bare electron-electron Coulomb repulsion). The latter case applies to the quantum criticality in the Hertz-Millis-based description [30–32]. In this scenario, in the clean limit, only specific sections of the Fermi surface lose quasiparticle-like behavior (the so-called "hotspots") [33, 34] whereas the Fermi liquid description remains valid across the remainder of the Fermi surface, dominating transport properties and leaving the Fano factor intact. In contrast, zero momentum order parameter fluctuations – the kind relevant for ferromagnetism, Ising-nematic and excitonic orders – render the entire Fermi surface "hot" [30], even though their contributions to the electrical resistivity is expected to be superlinear in temperature. It is desirable to construct the Boltzmann-Langevin equations suitable for the study of shot noise in coupled electron-boson systems without assuming equilibrium bosons. Here, we do so and determine the shot noise. Our key conclusion is that a sufficiently strong electron-boson coupling restores the Fano factor to $F = \sqrt{3}/4$, as illustrated in Fig. 1(b). Our results support the suggestion [7, 8] that quantum criticality of beyond the Landau form [11–13] underlies the suppressed shot noise in $YbRh_2Si_2$, in a similar way that it causes a violation of the Wiedemann-Franz law [35].

Transport in electron-boson systems: Here, we consider metals with two distinct interacting degrees of freedom, one fermionic (electrons; ψ) and the other bosonic (phonons, collective soft modes, etc.; ϕ), with their interaction modeled by a Yukawa term, $\phi\psi^\dagger\psi$ [36] A universal description of the system in the presence of an external electromagnetic field, $\boldsymbol{E}$, which acts as a source terms, is given by

$$S = \int \mathrm{d}\tau\, \mathrm{d}\boldsymbol{r} \left\{ \mathcal{L}[\psi, \phi] + V(\boldsymbol{r})\psi^\dagger\psi + ie\boldsymbol{A}(\tau, \boldsymbol{r}) \cdot \psi^\dagger \boldsymbol{\nabla}\psi \right\}, \tag{1}$$

where $\mathcal{L}[\psi, \phi] = \psi^\dagger[\partial_\tau - H_0(\boldsymbol{\nabla})]\psi - \phi^\dagger\left[\partial_\tau^2 + c^2\nabla^2\right]\phi + \phi\psi^\dagger g(\boldsymbol{\nabla})\psi + u_\psi\left(\psi^\dagger\psi\right)^2 + u_\phi|\phi|^4$, $V(\boldsymbol{r})$ is a random potential with $\langle V(\boldsymbol{r})V(\boldsymbol{r}')\rangle \propto \delta(\boldsymbol{r} - \boldsymbol{r}')$ which is responsible for elastic scatterings among the electrons, $g(\boldsymbol{\nabla})$ is a coupling function that controls the interaction between ψ and ϕ, $\boldsymbol{A}$ is an external electromagnetic field such that the applied electric field $\boldsymbol{E} = -\partial_t\boldsymbol{A}$. We will work in the regime where the self-interaction among the bosons is weak; henceforth, we set $u_\phi = 0$ and simplify notation by setting $u_\psi \to u$. The diagrammatic representation of the remaining vertices is shown in Appendix C. Here, the source of the Yukawa vertex is the four-fermion interaction channel that produces soft collective modes as the system is tuned towards a quantum critical point. The remaining four-fermion interaction channels are represented by the $u(\psi^\dagger\psi)^2$ term. Thus, away from the critical point, while both interaction channels suppress the quasiparticle weight, the development of non-Fermi liquid correlations solely result from the Yukawa vertex [30].

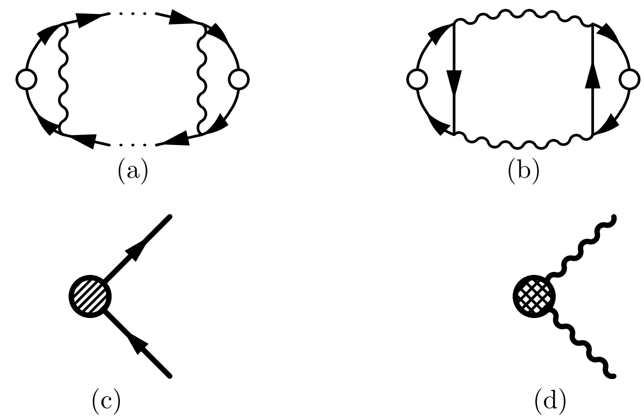

FIG. 2. Scattering processes contributing to the electrical conductivity. In diagrams of type (a) the external frequency-momentum can be carried entirely by electronic propagators. Here, one or more of the boson lines can be exchanged for the dashed lines representing four-fermion vertices [c.f. Appendix C]. For diagrams of type (b), both virtual bosons and electrons carry external frequency-momentum. These processes become important in the drag regime, as explained in the text. (c) and (d) are the renormalized current vertices that capture the scattering of electrons and bosons by the external photon, the thick straight (wavy) lines represent the fully renormalized electron (boson) propagators.

The conductivity tensor is given by $\sigma_{ij} = \left\langle(\psi^\dagger\partial_i\psi)(\psi^\dagger\partial_j\psi)\right\rangle$, which receives quantum corrections from the interaction terms in $\mathcal{L}$. Following Holstein [37], we compute σ_{ij} at finite g and u. Two classes of diagrams contribute to σ_{ij}. The first class of diagrams is exemplified by processes depicted in Figs. 2(a), where the external frequency-momentum can be carried entirely by electronic virtual excitations. The second class of diagrams, represented by Fig. 2(b), constitute scattering processes where the external frequency-momentum must necessarily be carried by both virtual electrons and bosons. As a result, in scattering processes of the former (latter) category the bosons are at equilibrium (out of equilibrium), which makes the latter class of diagrams to become important in the drag regime where both the electrons and the bosons are out of equilibrium [37].

While computing σ_{ij} in the drag regime, it is convenient to view the renormalizations to the external-source vertex (c.f., Appendix C) as a self consistent solution to a pair of coupled equations for renormalizations to the current-vertices, one for each type of current-vertex in Figs. 2(c) and (d). These equations are represented diagrammatically as

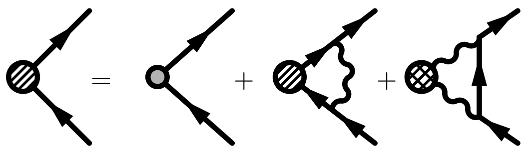

(2)

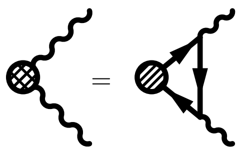

(3)

In Eq. (2) the quantum corrections are split into three categories: the first term is the renormalized current vertex for the electrons due to the four-fermion scatterings, the second term contains additional corrections purely due to the Yukawa vertex, and the final term encodes the feedback from the boson-current vertex. Since the bosons are not charged, they do not directly couple with the external gauge field. Consequently, the quantum corrections in Eq. (3) are generated only through the renormalized electron-current vertex. We note that in Eqs. (2) and (3) the propagators are fully dressed by u, g, and V appearing in (1), which implies that the fermionic excitations that contribute to the above processes are not necessarily quasiparticles. We have assumed that the system is in the regime where the Migdal's theorem applies such that the vertex corrections from the Yukawa vertex can be neglected and, in addition, the spectral functions contain dispersive peaks.

The coupled equations above can be utilized to obtain a relationship between the electron and boson distribution functions [37], as described in Appendix A.

In the limit $\Omega \to 0$, Eqs. (A1) and (A2) lead to a set of coupled Boltzmann equations for the electrons and bosons with electron-boson (I_{eb}) and boson-electron (I_{be}) collision integtals. For completeness, we add collision integrals resulting electron-electron (I_{ee}), boson-boson (I_{bb}), electron-impurity scatterings (I_{imp}) and Langevin source $\delta J^{ext}(x,k,t)$ [38] This procedure leads to the following coupled Boltzmann-Langevin equations:

$$\begin{aligned}
&\hat{\mathcal{L}}_\psi f(x,k) + I_{imp}(x,k) + I_{ee}(x,k) + I_{eb}(x,k) = \delta J^{ext} \\
&\hat{\mathcal{L}}_\phi N(x,q) + I_{bb}(x,q) + I_{be}(x,q) = 0
\end{aligned} \tag{4}$$

where

$$\begin{aligned}
&\hat{\mathcal{L}}_\psi f(x,\boldsymbol{k}) \\
&= \left[\partial_t + v_x\partial_x + (e\boldsymbol{E} - \sum_{\boldsymbol{k}'} U_{\boldsymbol{k},\boldsymbol{k}'}\partial_x \delta f_{\boldsymbol{k}'})\cdot\partial_{\boldsymbol{k}}\right] f(x,\boldsymbol{k})
\end{aligned} \tag{5}$$

$$\hat{\mathcal{L}}_\phi N(x,\boldsymbol{q}) = (\partial_t + c_x\partial_x)N(x,\boldsymbol{q}) \tag{6}$$

and $v_x = \partial\epsilon_k/\partial k_x$ and $c_x = \partial\omega_q/\partial q_x$ are the group velocities of the electronic and bosonic excitations, respectively, and the fermion distribution function f here equals f^+ introduced above. In addition, $U_{\boldsymbol{k},\boldsymbol{k}'}$ describes the effective electron-electron interaction, δJ^{ext} is the extraneous electronic flux for the description of electronic fluctuations and shot noise [8, 39]. In the correlated regime, where the electron-electron scattering length l_{ee} is much smaller than the system size L, strong electron scattering significantly shapes the nonequilibrium fermion distribution. This distribution, which was derived in our previous work[8], has the following form: $f(x,k) = f_F(\epsilon_{\boldsymbol{k}}, T_e(x)) + eEv_x\tau\partial_\epsilon f_F$, where $f_F(\epsilon_{\boldsymbol{k}}, T_e)$ is the Fermi Dirac distribution function with the electron energy $\epsilon_{\boldsymbol{k}} = \epsilon^0_{\boldsymbol{k}} + \sum_{\boldsymbol{p}'} U_{\boldsymbol{k},\boldsymbol{k}'}\delta f_{\boldsymbol{k}'}$ and temperature T_e. The first term in this expression, symmetric in momentum space, is critical for determining the characteristics of shot noise, while the second, antisymmetric term predominantly influences the current behavior.

Shot noise: When the impurity scattering is dominant over inelastic scatterings, the shot noise can be expressed as [8, 39]:

$$S = \frac{4G}{L}\int_{-L/2}^{L/2} dx \int d\epsilon f(x,\epsilon)(1 - f(x,\epsilon)) = 4G\bar{T}_e \tag{7}$$

where $\bar{T}_e = \frac{1}{L}\int_{-L/2}^{L/2} dx T_e(x)$ is the averaged nonequilibrium temperature. The Fano factor, defined as the ratio between noise and current, could be expressed as follows,

$$F = \frac{S}{2eGV} = 2\bar{\Theta}_e \tag{8}$$

where $\bar{\Theta}_e \equiv \bar{T}_e/eV$ denotes for the dimensionless averaged temperature. In the absence of any electron-boson coupling, the Fano factor F is $1/3$ for non-interacting electrons[39] and $\sqrt{3}/4$ for hot electrons with strong electron-electron collisions[27, 40]. It holds true even in the context of a strongly correlated Fermi liquid where the Landau parameters are considered to be large [8].

When the electron-boson coupling is present, the electrons and bosons will exchange energy and momentum during electron-boson scattering. Consequently, the temperatures of the electrons (T_e) and bosons (T_b) evolve, which in turn affects the characteristics of the shot noise. To accurately track this evolution, it is necessary to solve the coupled Boltzmann-Langevin equations for both electrons and bosons. In this study, we consider the case where bosons deviate from global equilibrium due to interactions with nonequilibrium electrons, and assume they achieve local equilibrium in the steady state due to scattering with electrons. This local equilibrium is characterized by a Bose distribution function $n_B(\omega, T_b(x))$, where $T_b(x)$ denotes the locally defined temperature at position x within the sample.

To investigate the evolution of T_e and T_b, we derive the diffusion equations for electrons and bosons. They are obtained by splitting their nonequilibrium distributions into symmetric and antisymmetric part, and substituting equation for the antisymmetric part into symmetric part (for details see the Appendix D):

$$D\partial_x^2 f(\epsilon, T_e) + I_{eb} = 0 \tag{9}$$

$$\partial_x^2 n_B(\omega, T_b) = \frac{d}{c^2\tau_{be}}\left(\frac{1}{\tau_{be}} + \frac{1}{\tau_{bb}}\right)[n_B(\omega, T_b) - n_B(\omega, T_e)] \tag{10}$$

where

$$I_{eb} = \int d\omega M(\omega)[2f(\epsilon, T_e) - f(\epsilon - \omega, T_e) - f(\epsilon + \omega, T_e)] \\ [n_B(\omega, T_e) - n_B(\omega, T_b)] \tag{11}$$

where $M(\omega) = \frac{\lambda_{eb}\omega^{n+d-2}}{2\pi v_F \omega_D^n c^{d-1}}$, $\frac{1}{\tau_{be}} = 4\pi N_F \lambda_{eb} \frac{c}{v_F}\left(\frac{\omega}{\omega_D}\right)^n$. Here, d is the space dimension, $n = 1$ describes the scaling of the Yukawa coupling with Goldstone bosons (e.g. phonons and AFM magnons), and $n = 0$ corresponds to the Yukawa coupling with critical bosons (e.g. collective soft modes of the Hubbard-Stratonovich field). The inverse boson-boson scattering time, represented by $1/\tau_{bb}$, is assumed to be negligible relative to $1/\tau_{be}$. Multiplying Eq.(9) with ϵ and integrate with ϵ, also multiplying Eq.(10) with ω^{d-n} and integrate with ω, one gets:

$$L^2\partial_x^2\Theta_e^2 + \frac{6}{\pi^2} = \gamma_e(\Theta_e^{d+n+1} - \Theta_b^{d+n+1}) \tag{12}$$

$$L^2\partial_x^2\Theta_b^{d-n+1} = \gamma_b(\Theta_b^{d+n+1} - \Theta_e^{d+n+1}) \tag{13}$$

where $\Theta_{e(b)}$, the dimensionless temperature for electrons (bosons), and the parameters γ_e and γ_b are defined as follows

$$\Theta_{e(b)} = T_{e(b)}/eV; \quad \gamma_e = L^2/l_{eb}^2; \quad \gamma_b = L^2/l_{be}^2, \tag{14}$$

with $l_{eb}^{-1} \equiv l_{e\leftarrow b}^{-1} = \sqrt{\frac{6\zeta(d+n+1)\Gamma(d+n+1)}{2\pi^3 v_F c^{d-1}\omega_D^n D}\lambda_{eb}(eV)^{d+n-1}}$ and $l_{be}^{-1} \equiv l_{b\leftarrow e}^{-1} = \sqrt{\frac{8d\pi^2 N_F^2}{v_F^2\omega_D^{2n}}\frac{\zeta(d+n+1)\Gamma(d+n+1)}{\zeta(d-n+1)\Gamma(d-n+1)}\lambda_{eb}^2(eV)^{2n}}$. $\zeta(x)$ and $\Gamma(x)$ denote the Riemann zeta function and the Gamma function, respectively. $\gamma_{e(b)}$ are dimensionless quantities that characterize the energy relaxations of electrons (bosons) due to interactions with bosons (electrons), respectively. The terms l_{eb} and l_{be} denote the electron-boson and boson-electron relaxation lengths, respectively. Specifically, l_{eb} measures the distance electrons can travel without energy relaxation due to bosons, and l_{be} similarly applies for bosons relative to electrons.

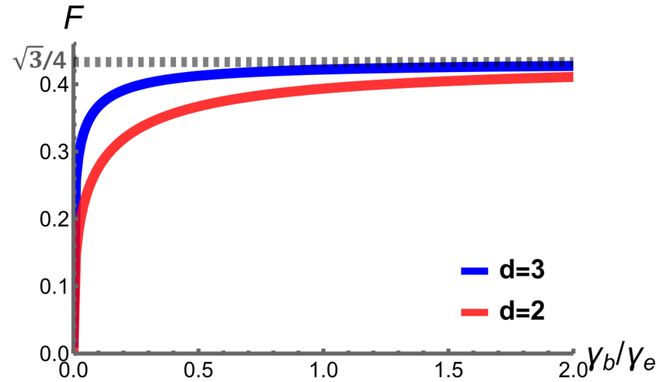

FIG. 3. Fano factor F as a function of the ratio $\gamma_b/\gamma_e \propto \lambda_{eb}$, in the electron-boson drag regime for critical bosons ($n = 0$), where $T_e(x) = T_b(x)$. This regime is characterized by either $\gamma_e \gg 1$ or $\gamma_b \gg 1$.

We note that the electron-boson relaxation length l_{eb} differs from the electron-boson scattering length used in the context of resistivity (e.g., Bloch's law for acoustic phonons), where the latter is derived from the linearized electron-boson collision integral assuming that bosons are in equilibrium. We further note that the ratio $\gamma_b/\gamma_e \propto \lambda_{eb}$, the electron-boson coupling at the Yukawa vertex.

Multiplying Eq.(13) with γ_e/γ_b and sum with Eq.(12), one can get an exact relation between the two temperatures:

$$\Theta_e^2 + \frac{\gamma_e}{\gamma_b}\Theta_b^{d-n+1} = \frac{6}{\pi^2}\left[\frac{1}{8} - \frac{1}{2}\left(\frac{x}{L}\right)^2\right] \tag{15}$$

where we utilized the zero temperature conditions at two boundaries: $T_e(\pm\frac{L}{2}) = T_b(\pm\frac{L}{2}) = 0$. This relation captures the *conservation law* of heat transfer between electrons and bosons under local equilibrium conditions. Here, the second term in Eq.(15) can be neglected when $\gamma_e \ll \gamma_b$, corresponding to $l_{be} \ll l_{eb}$. In this regime, the electrons stay hot, resulting in Fano factor $F = \sqrt{3}/4$. Conversely, when $\gamma_b \ll \gamma_e$, or equivalently $l_{eb} \ll l_{be}$, the temperature of the bosons, $\Theta_b \to 0$. This occurs because in the absence of significant scattering from electrons ($1/\tau_{be} = 0$), bosons remain in global equilibrium.

We investigate the regime where $\gamma_e \gg 1$ or $\gamma_b \gg 1$, which arises when the electron-boson or boson-electron scattering is sufficiently strong such that $L \gg l_{eb}$ or l_{be}. The strong drag between electrons and bosons equalizes their temperatures, leading to:

$$\Theta_e = \Theta_b \tag{16}$$

as seen from Eqn. (12 or (13) at leading order. Under such drag regime, one can get analytic solutions for Θ_e after combining Eq. (16) with Eq. (15). We summarize these results in Table (I) and plot them as functions of γ_b/γ_e in Fig. 3. We note that our analytical results are fully supported by the direct numerical solution to Eqs. (12, 13).

$\Theta_e^{(d-n)}(x)$	$n=0$	$n=1$
$d=2$	$\Theta^{(2)}\left(\frac{\gamma_b}{\gamma_e}, \Theta_{0e}\right)$	$\sqrt{\frac{\gamma_b}{\gamma_e+\gamma_b}}\Theta_{0e}$
$d=3$	$\frac{1}{\sqrt{2}}\left(\sqrt{\frac{\gamma_b^2}{\gamma_e^2}+\frac{4\gamma_b}{\gamma_e}\Theta_{0e}^2}-\frac{\gamma_b}{\gamma_e}\right)^{\frac{1}{2}}$	$\Theta^{(2)}\left(\frac{\gamma_b}{\gamma_e}, \Theta_{0e}\right)$

TABLE I. Table of local temperature for electrons coupled with critical ($n=0$) and Goldstone ($n=1$) bosons in two ($d=2$) and three ($d=3$) dimensions in the limit $\gamma_e \gg 1$. $\Theta_{0e}(x) = \sqrt{\frac{3}{4\pi^2}\left[1-\left(\frac{2x}{L}\right)^2\right]}$ is the local temperature of hot electrons without electron-boson couplings, which leads to $F(\lambda_{eb}=0) = \frac{\sqrt{3}}{4}$. The form of $\Theta^{(2)}$ is shown in Appendix E.

Discussion: Fig. 3 is the central result of our work. Note that $\gamma_b/\gamma_e \propto \lambda_{\rm eb}$. When the electron-boson coupling $\lambda_{\rm eb}$ is small, $l_{eb} \ll L, l_{be}$, and the Fano factor F goes below $\sqrt{3}/4$. By contrast, when the electron-boson couping is adequately large, as we expect for the cases where the bosons correspond to collective excitations of the electrons, the Fano factor is restored to $\sqrt{3}/4$. This qualitative trend is illustrated in Fig. 1(b).

To summarize, in this paper we study the shot noise in a coupled electron-boson system when the bosons are allowed to go out of equilibrium due to their interactions with the electrons. We construct the coupled Boltzmann-Langevin equations. We show that adequate electron-boson couplings restore the Fano factor to its Fermi liquid value. Our results are important for understanding the reduced shot noise observed in quantum critical heavy fermion metals and beyond, pointing to the quasiparticles being lost from the beyond-Landau form of quantum criticality as the underlying mechanism.

ACKNOWLEDGMENTS

We thank Matt Foster, Joel Moore, Doug Natelson, Silke Paschen, Sri Raghu, Subir Sachdev and Tsz Chun Wu for useful discussions. This work has primarily been supported by the National Science Foundation under Grant No. DMR-2220603 (Y.W. and S.S.), Air Force Office of Scientific Research under Grant No. FA9550-21-1-0356 (C.S.), and by the Robert A. Welch Foundation Grant No. C-1411 (Q.S.) and the Vannevar Bush Faculty Fellowship ONR-VB N00014-23-1-2870 (Q.S.). SS and QS acknowledge the hospitality of the Kavli Institute for Theoretical Physics, UCSB, supported in part by grant NSF PHY-2309135.

[1] Lev Davidovich Landau and Evgenii Lifshitz, *Course of theoretical physics* (Elsevier, 2013).
[2] S. Paschen and Q. Si, “Quantum phases driven by strong correlations,” Nat. Rev. Phys. **3**, 9 (2021).
[3] Haoyu Hu, Lei Chen, and Qimiao Si, “Quantum critical metals: Dynamical planckian scaling and loss of quasiparticles,” arXiv preprint arXiv:2210.14183 (2022).
[4] Philip W. Phillips, Nigel E. Hussey, and Peter Abbamonte, “Stranger than metals,” Science **377**, eabh4273 (2022).
[5] Ya M Blanter and Markus Buttiker, “Shot noise in mesoscopic conductors,” Physics reports **336**, 1–166 (2000).
[6] Kensuke Kobayashi and Masayuki Hashisaka, “Shot noise in mesoscopic systems: From single particles to quantum liquids,” Journal of the Physical Society of Japan **90**, 102001 (2021), https://doi.org/10.7566/JPSJ.90.102001.
[7] Liyang Chen, Dale T Lowder, Emine Bakali, Aaron Maxwell Andrews, Werner Schrenk, Monika Waas, Robert Svagera, Gaku Eguchi, Lukas Prochaska, Yiming Wang, *et al.*, “Shot noise in a strange metal,” Science **382**, 907–911 (2023).
[8] Yiming Wang, Chandan Setty, Shouvik Sur, Liyang Chen, Silke Paschen, Douglas Natelson, and Qimiao Si, “Shot noise as a characterization of strongly correlated metals,” arXiv preprint arXiv:2211.11735 (2022).
[9] Tsz Chun Wu and Matthew S. Foster, “Suppression of shot noise in a dirty marginal fermi liquid,” (2023), arXiv:2312.03071 [cond-mat.str-el].
[10] Alexander Nikolaenko, Subir Sachdev, and Aavishkar A. Patel, “Theory of shot noise in strange metals,” Phys. Rev. Res. **5**, 043143 (2023).
[11] Q. Si, S. Rabello, K. Ingersent, and J. Smith, “Locally critical quantum phase transitions in strongly correlated metals,” Nature **413**, 804–808 (2001).
[12] P Coleman, C Pépin, Q. Si, and R. Ramazashvili, “How do Fermi liquids get heavy and die?” J. Phys. Cond. Matt. **13**, R723 (2001).
[13] T. Senthil, M. Vojta, and S. Sachdev, “Weak magnetism and non-fermi liquids near heavy-fermion critical points,” Phys. Rev. B **69**, 035111 (2004).
[14] Steffen Wirth and Frank Steglich, “Exploring heavy fermions from macroscopic to microscopic length scales,” Nat. Rev. Mater. **1**, 16051 (2016).
[15] Stefan Kirchner, Silke Paschen, Qiuyun Chen, Steffen Wirth, Donglai Feng, Joe D. Thompson, and Qimiao Si, “Colloquium: Heavy-electron quantum criticality and single-particle spectroscopy,” Rev. Mod. Phys. **92**, 011002 (2020).
[16] S. Paschen, T. Lühmann, S. Wirth, P. Gegenwart, O. Trovarelli, C. Geibel, F. Steglich, P. Coleman, and Q. Si, “Hall-effect evolution across a heavy-fermion quantum critical point,” Nature **432**, 881 (2004).
[17] S. Friedemann, N. Oeschler, S. Wirth, C. Krellner, C. Geibel, F. Steglich, S. Paschen, S. Kirchner, and Q. Si, “Fermi-surface collapse and dynamical scaling near a quantum-critical point,” PNAS **107**, 14547–14551 (2010).
[18] H. Shishido, R. Settai, H. Harima, and Y. Ōnuki, “A drastic change of the Fermi surface at a critical pressure in $CeRhIn_5$: dHvA study under pressure,” J. Phys. Soc. Jpn. **74**, 1103–1106 (2005).

[19] A. Schröder, G. Aeppli, R. Coldea, M. Adams, O. Stockert, H. v. Löhneysen, E. Bucher, R. Ramazashvili, and P. Coleman, "Onset of antiferromagnetism in heavy-fermion metals," Nature **407**, 351–355 (2000).

[20] M. C. Aronson, R. Osborn, R. A. Robinson, J. W. Lynn, R. Chau, C. L. Seaman, and M.B. Maple, "Non-Fermi-liquid scaling of the magnetic response in $UCu_{5-x}Pd_x$ ($x = 1, 1.5$)," Phys. Rev. Lett. **75**, 725–728 (1995).

[21] L. Prochaska, X. Li, D. C. MacFarland, A. M. Andrews, M. Bonta, E. F. Bianco, S. Yazdi, W. Schrenk, H. Detz, A. Limbeck, Q. Si, E. Ringe, G. Strasser, J. Kono, and S. Paschen, "Singular charge fluctuations at a magnetic quantum critical point," Science **367**, 285–288 (2020).

[22] GV Chester and A Thellung, "The law of wiedemann and franz," Proceedings of the Physical Society (1958-1967) **77**, 1005 (1961).

[23] C Castellani, C DiCastro, G Kotliar, PA Lee, and G Strinati, "Thermal conductivity in disordered interacting-electron systems," Physical review letters **59**, 477 (1987).

[24] K Kadowaki and SB Woods, "Universal relationship of the resistivity and specific heat in heavy-fermion compounds," Solid state communications **58**, 507–509 (1986).

[25] MJ Rice, "Electron-electron scattering in transition metals," Physical Review Letters **20**, 1439 (1968).

[26] Andrew H Steinbach, John M Martinis, and Michel H Devoret, "Observation of hot-electron shot noise in a metallic resistor," Physical review letters **76**, 3806 (1996).

[27] KE Nagaev, "Influence of electron-electron scattering on shot noise in diffusive contacts," Physical Review B **52**, 4740 (1995).

[28] CWJ Beenakker and M Buttiker, "Suppression of shot noise in metallic diffusive conductors," Physical Review B **46**, 1889 (1992).

[29] Akira Shimizu and Masahito Ueda, "Effects of dephasing and dissipation on quantum noise in conductors," Physical review letters **69**, 1403 (1992).

[30] Sung-Sik Lee, "Recent developments in non-fermi liquid theory," Annual Review of Condensed Matter Physics **9**, 227–244 (2018).

[31] Shouvik Sur and Sung-Sik Lee, "Quasilocal strange metal," Physical Review B **91**, 125136 (2015).

[32] Max A Metlitski and Subir Sachdev, "Quantum phase transitions of metals in two spatial dimensions. ii. spin density wave order," Physical Review B **82**, 075128 (2010).

[33] R Hlubina and TM Rice, "Resistivity as a function of temperature for models with hot spots on the fermi surface," Physical Review B **51**, 9253 (1995).

[34] A Rosch, "Interplay of disorder and spin fluctuations in the resistivity near a quantum critical point," Physical Review Letters **82**, 4280 (1999).

[35] Heike Pfau, Stefanie Hartmann, Ulrike Stockert, Peijie Sun, Stefan Lausberg, Manuel Brando, Sven Friedemann, Cornelius Krellner, Christoph Geibel, Steffen Wirth, *et al.*, "Thermal and electrical transport across a magnetic quantum critical point," Nature **484**, 493–497 (2012).

[36] Bose-Fermi systems that do not feature a Yukawa coupling arise in ultracold atomic systems, which is beyond the scope of this paper.

[37] T Holstein, "Theory of transport phenomena in an electron-phonon gas," Annals of Physics **29**, 410–535 (1964).

[38] We note that this can be done systematically following Refs. [8, 41].

[39] KE Nagaev, "On the shot noise in dirty metal contacts," Physics Letters A **169**, 103–107 (1992).

[40] VI Kozub and AM Rudin, "Shot noise in mesoscopic diffusive conductors in the limit of strong electron-electron scattering," Physical Review B **52**, 7853 (1995).

[41] O Betbeder-Matibet and P Nozieres, "Transport equation for quasiparticles in a system of interacting fermions colliding on dilute impurities," Annals of Physics **37**, 17–54 (1966).

[42] For a critical boson coupled to electrons it is customary to retain the most relevant part of the electron-boson coupling function in the sense of renormalization group, and g is momentum independent. By contrast, for phonon-electron coupling g is generically momentum dependent, since phonons are Goldstone modes.

[43] We note that this can be done systematically following Refs. [8, 41].

Appendix A: Coupled Boltzmann equations

The coupled equations (2,3) of the main text can be utilized to obtain a relationship between the electron and boson distribution functions [37],

$$i(\mathbf{Q}\cdot\mathbf{v}_k-\Omega)\Phi_k = v_k + 2\pi\sum_{\mathbf{q},\pm}|g_q|^2\Bigg[(\Phi_{k\pm q}-\Phi_k\mp n_q)\left(\frac{f_F^{\mp}(\epsilon_{k\pm q}+\Omega)+f_F^{\mp}(\epsilon_{k\pm q})}{2}+n_B(\omega_q)\right)\delta(\epsilon_k-\epsilon_{k+q}+\omega_q)$$
$$+\frac{i}{2\pi}\mathfrak{P}\left(\frac{1}{\epsilon_k-\epsilon_{k\pm q}\pm\omega_q}\right)\left(f_F^{\mp}(\epsilon_{k\pm q}+\Omega)-f_F^{\mp}(\epsilon_{k\pm q})\right)(\Phi_{k\pm q}-\Phi_k)\Bigg] \tag{A1}$$

$$i(\mathbf{Q}\cdot\nabla_q\omega_q-\Omega)n_q = 2\pi\sum_k|g_q|^2\delta(\epsilon_k+\omega_q-\epsilon_{k+q})\left[-f_F^-(\epsilon_k+\omega_q)+f_F^-(\epsilon_k)\right][\Phi_{k+q}-\Phi_k-n_q]\,. \tag{A2}$$

Here, we have set $\hbar=1$, v_k is the magnitude of the renormalized fermion-current vertex due to local coulomb interactions, $(\Omega,\mathbf{Q})$ are the frequency-momentum of the external electromagnetic field, $\boldsymbol{A}$, $f_F^{\pm}(x)$ is the Fermi-Dirac distribution function for the occupied and vacant states, $n_B(x)$ is the Bose distribution function, $\Phi_k = \left[f_k-f_F^-(\epsilon_k)\right]/\left[eE\partial_{\epsilon_k}f_F^-(\epsilon_k)\right]$ and $n_q=\left[N_q-n_B(\omega_q)\right]/\left[eE\partial_{\omega_q}n_B(\omega_q)\right]$ with f_k and N_q being the full fermion and boson distribution functions, respectively, $\mathfrak{P}(x)$ denotes the principal value, g_q is the Fourier components of the Yukawa coupling [42], and ϵ_k and ω_q are the electron and boson dispersions respectively. We note that the Thomas-Fermi screened temporal part of the electromagnetic gauge field can also participate in Boltzmann transport as an independent bosonic mode. Here, we assume the temperature window is sufficiently smaller than the Thomas-Fermi screening scale, such that the temporal part of the electromagnetic gauge field does not participate in transport. We describe the case when the spectral functions are sharp, though we expect our analysis to remain valid provided that the spectral functions are sharp enough to display dispersive peaks.

In the limit $\Omega\to 0$, Eqs. (A1) and (A2) leads to a set of coupled Boltzmann equations for the electrons and bosons with electron-boson (I_{eb}) and boson-electron (I_{be}) collision integtals. For completeness, we add collision integrals resulting electron-electron (I_{ee}), boson-boson (I_{bb}), , electron-impurity scatterings (I_{imp}) and Langevin source $\delta J^{ext}(x,k,t)$ [43]. This leads to the coupled Boltzmann-Langevin equations given in Eq. (4) of the main text.

Appendix B: From coupled vertex corrections to Boltzmann equations

In this section we outline the path from Eqs. (A1) and (A2) in the previous Appendix to the coupled Boltzmann equations. Here, Φ_k and n_q parameterize the deviations from the equilibrium fermion and boson distribution functions, respectively,

$$f_k = f_F^-(\epsilon_k)+eE\Phi_k\partial_{\epsilon_k}f_F^-(\epsilon_k);\qquad N_q=n_B(\omega_q)+eEn_q\partial_{\omega_q}n_B(\omega_q). \tag{B1}$$

In the limit $\Omega\to 0$ we obtain

$$i\mathbf{Q}\cdot\mathbf{v}_k\Phi_k = v_k+2\pi\sum_{\mathbf{q},s=\pm}W_s(k,q)(\Phi_{k+sq}-\Phi_k-sn_q)\left(f_F^{-s}(\epsilon_{k+sq})+n_B(\omega_q)\right) \tag{B2}$$

$$i\mathbf{Q}\cdot\nabla_q\omega_q n_q = 2\pi\sum_k W_+(k,q)\left[-f_F^-(\epsilon_k+\omega_q)+f_F^-(\epsilon_k)\right][\Phi_{k+q}-\Phi_k-n_q] \tag{B3}$$

where we have defined the transition probability

$$W_s(k,q)=2\pi|g_q|^2\delta(\epsilon_k-\epsilon_{k+q}+s\omega_q) \tag{B4}$$

We multiply both sides of Eq. (B2) [Eq. (B3)] by $eE\partial_{\epsilon_k}f_F(\epsilon_k)$ $[eE\partial_{\omega_q}n_B(\omega_q)]$, and add $i\mathbf{Q}\cdot\mathbf{v}_kf_F$ $[i\mathbf{Q}\cdot\mathbf{v}_kn_B]$ to obtain the Boltzmann equations in the main text.

Appendix C: Bare vertices

Here we specify the bare vertices associated with interaction terms in Eq(1) of the main text.

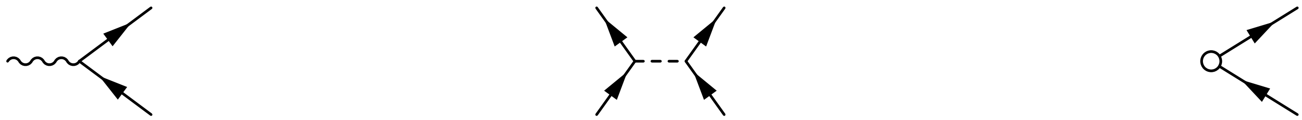

(a) (b) (c)

FIG. 4. Graphical representation of the three vertices that contribute to electrical conductivity. (a) The electron-boson vertex; (b) the four-fermion vertex; (c) the external source vertex representing the direct coupling between an applied electromagnetic field and the electron current.

Appendix D: Boltzmann equations for electron-boson coupled systems

We study the coupled Boltzmann equations for electrons and bosons:

$$\mathcal{L}f(x,k) + I_{imp}(x,k) + I_{ee}(x,k) + I_{e-ph}(x,k) = 0 \tag{D1}$$

$$c_x\partial_x N(x,q) + I_{ph-ph}(x,q) + I_{ph-e}(x,q) = 0 \tag{D2}$$

where the collision integrals are given by

$$I_{imp}(x,k) = \sum_{k'} W(kk')[f(x,k)(1-f(x,k')) - f(x,k')(1-f(x,k))], \tag{D3}$$

$$I_{ee}(x,k) = \sum_{2,3,4} \widetilde{W}(12;34)\delta_{\boldsymbol{k}+\boldsymbol{k}_2,\boldsymbol{k}_3+\boldsymbol{k}_4}\delta(\epsilon+\epsilon_2-\epsilon_3-\epsilon_4)[f_3f_4(1-f_1)(1-f_2) - f_1f_2(1-f_3)(1-f_4)], \tag{D4}$$

$$\begin{aligned} I_{eb}(x,k) =& 2\pi\sum_{\boldsymbol{q}} |g_{\boldsymbol{q}}|^2 \left\{[1-f(x,\boldsymbol{k})]f(x,\boldsymbol{k}+\boldsymbol{q})[1+N(x,\boldsymbol{q})] - f(x,\boldsymbol{k})[1-f(x,\boldsymbol{k}+\boldsymbol{q})]N_\lambda(x,\boldsymbol{q})\right\}\delta(\epsilon_{\boldsymbol{k}}+\omega_{\boldsymbol{q}\lambda}-\epsilon_{\boldsymbol{k}+\boldsymbol{q}}) \\ &+ |g_{\boldsymbol{q}}|^2\left\{[1-f(x,\boldsymbol{k})]f(x,\boldsymbol{k}+\boldsymbol{q})N(x,-\boldsymbol{q}) - f(x,\boldsymbol{k})[1-f(x,\boldsymbol{k}+\boldsymbol{q})][1+N_\lambda(x,\boldsymbol{q})]\right\}\delta(\epsilon_{\boldsymbol{k}}-\omega_{-\boldsymbol{q}\lambda}-\epsilon_{\boldsymbol{k}-\boldsymbol{q}}) \end{aligned} \tag{D5}$$

$$I_{be}(x,q) = 4\pi\sum_{\boldsymbol{k}} |g_{\boldsymbol{q}}|^2\left\{[1+N(x,\boldsymbol{q})]f(x,\boldsymbol{k}+\boldsymbol{q})[1-f(x,\boldsymbol{k})] - N(x,\boldsymbol{q})[1-f(x,\boldsymbol{k}+\boldsymbol{q})]f(x,\boldsymbol{k})\right\}\delta(\epsilon_{\boldsymbol{k}+\boldsymbol{q}}-\omega_{\boldsymbol{q}\lambda}-\epsilon_{\boldsymbol{k}}), \tag{D6}$$

and $c_x = \frac{\partial\omega_q}{\partial q_x} = \frac{cq_x}{q}$ is the group velocity of bosons. In these collision integals, $W(pp')$ and $\widetilde{W}(12;34)$ are the scattering probability for electron-impurity and electron-electron collisions respectively, and $|g_q|^2 = \lambda_{eb}\left(\frac{\omega}{\omega_D}\right)^n$, where $n=1$ denotes for the Yukawa coupling with Goldstone bosons (e.g. phonons and AFM magnons), and $n=0$ denotes for the Yukawa coupling with critical bosons (e.g. collective soft modes of the Hubbard-Stratonovich field).

When $l_{ee} \ll L$, the Fermi distribution has the following local equilibrium form:

$$f(x,\boldsymbol{k}) = f_F(\epsilon_{\boldsymbol{k}}, T_e(x)) + e\boldsymbol{E}\cdot\boldsymbol{v}_{\boldsymbol{k}}\tau\frac{\partial f_F}{\partial\epsilon_k} \approx f_F(\epsilon_{\boldsymbol{k}} - e\boldsymbol{E}\cdot\boldsymbol{v}_{\boldsymbol{k}}\tau, T_e(x)) \tag{D7}$$

For simplicity, we assume the velocity of fermions is equal to the Fermi velocity $v_k = v_F$.

The form of I_{be} can be simplified with the help of Eqn.D7,

$$I_{be}(x,q) = 4\pi|g_q|^2[n_B(\omega_q, T_e(x)) - N(x,q)]\sum_k [f(\epsilon_k - eEv_F\tau) - f(\epsilon_k+\omega_q - eEv_F\tau)]\delta(\epsilon_{\boldsymbol{k}+\boldsymbol{q}}-\omega_{\boldsymbol{q}\lambda}-\epsilon_{\boldsymbol{k}}) \tag{D8}$$

$$= 4\pi N_F|g_q|^2\frac{c}{v_F}[n_B(\omega_q,T_e) - N(x,q)] \tag{D9}$$

where

$$\sum_k [f(\epsilon_k) - f(\epsilon_{k+q})]\delta(\omega - \epsilon_{k+q} + \epsilon_k) = -\frac{1}{\pi}Im[\sum_k \frac{1}{\omega - \epsilon_{k+q}+\epsilon_k + i\delta}] = N_F\frac{\omega}{v_Fq} \tag{D10}$$

The nonequilibrium boson distribution can be split into even and odd sectors:

$$N(x,q) = N_{even}(x,q) + N_{odd}(x,q) \tag{D11}$$

where $N_{even} = n_B(\omega_q, T_e)$ preserves under $q \to -q$, and $N_{odd}(x, q) = -N_{odd}(x, -q)$. Due to different parities, the boson Boltzmann equation is split into two equations:

$$c_x \partial_x N_{odd} = -[n_B(\omega_q, T_e) - N_{even}(x, q)]/\tau_{ph-e} \tag{D12}$$

$$c_x \partial_x N_{even} = N_{odd}(x, q)\left(\frac{1}{\tau_{be}(q)} + \frac{1}{\tau_{bb}(q)}\right) \tag{D13}$$

with $1/\tau_{be} = 4\pi N_F |g_q|^2 \frac{c}{v_F} = 4\pi N_F \lambda_{eb} \frac{c\omega^n}{v_F \omega_D^n}$. Combining Eqs.(D12,D13), one get

$$c_x^2 \partial_x^2 n_B(\omega_q, T_b(x)) = \frac{1}{\tau_{be}} \left(\frac{1}{\tau_{be}} + \frac{1}{\tau_{bb}}\right) [n_B(\omega_q, T_b(x)) - n_B(\omega_q, T_e(x))] \tag{D14}$$

where $c_x = \frac{\partial \omega_q}{\partial q_x} = \frac{c q_x}{q}$, $c_x^2 = \frac{1}{d} c^2$.

On the other hand, from the electron side, the collision integral can be simplified at leading order (we do not consider Umklapp scattering: $\boldsymbol{G} = 0$),

$$\begin{aligned} I_{eb}(x, k) =& 2\pi \sum_{\boldsymbol{q}} |g_{\boldsymbol{q}}|^2 \left\{[1 - f(x, \boldsymbol{k})] f(x, \boldsymbol{k}+\boldsymbol{q})[1 + N(x, \boldsymbol{q})] - f(x, \boldsymbol{k})[1 - f(x, \boldsymbol{k}+\boldsymbol{q})] N_\lambda(x, \boldsymbol{q})\right\} \delta(\epsilon_{\boldsymbol{k}} + \omega_{\boldsymbol{q}\lambda} - \epsilon_{\boldsymbol{k}+\boldsymbol{q}}) \\ &+ |g_{\boldsymbol{q}}|^2 \left\{[1 - f(x, \boldsymbol{k})] f(x, \boldsymbol{k}+\boldsymbol{q}) N(x, -\boldsymbol{q}) - f(x, \boldsymbol{k})[1 - f(x, \boldsymbol{k}+\boldsymbol{q})][1 + N_\lambda(x, \boldsymbol{q})]\right\} \delta(\epsilon_{\boldsymbol{k}} - \omega_{-\boldsymbol{q}\lambda} - \epsilon_{\boldsymbol{k}-\boldsymbol{q}}) \end{aligned} \tag{D15}$$

$$\begin{aligned} =& \int d\omega M(\omega) \left\{[1 - f(\epsilon_{\boldsymbol{k}}, T_e)] f(\epsilon_{\boldsymbol{k}} + \omega, T_e)[1 + n_B(\omega, T_b)] - f(\epsilon_{\boldsymbol{k}}, T_e))[1 - f(\epsilon_{\boldsymbol{k}} + \omega, T_e)] n_B(\omega, T_b)\right. \\ &\left. + [1 - f(\epsilon_{\boldsymbol{k}}, T_e)] f(\epsilon_{\boldsymbol{k}} - \omega, T_e) N(\omega, T_b) - f(\epsilon_{\boldsymbol{k}}, T_e)[1 - f(\epsilon_{\boldsymbol{k}} - \omega, T_e)][1 + N(\omega, T_b)]\right\} \end{aligned} \tag{D16}$$

$$= \int d\omega M(\omega)[2f(\epsilon_{\boldsymbol{k}}, T_e) - f(\epsilon_{\boldsymbol{k}} - \omega, T_e) - f(\epsilon_{\boldsymbol{k}} + \omega, T_e)][n_B(\omega, T_e) - n_B(\omega, T_b)], \tag{D17}$$

where

$$M(\omega) = 2\pi \int \frac{d^d \boldsymbol{q}}{(2\pi)^d} |g_q|^2 \delta(\omega - \omega_q) \delta(\epsilon_k + \omega_q - \epsilon_{k+q}). \tag{D18}$$

For parabolic electronic bands we have,

$$\omega_q + \epsilon_k - \epsilon_{k+q} = (c - v_F \cos\theta) q + \frac{q^2}{2m}. \tag{D19}$$

The form of $M(\omega)$ is dimensionality dependent. For small $\boldsymbol{q}$ in three dimensions

$$M(\omega) = \frac{1}{2\pi} \frac{\lambda}{v_F c^2 \omega_D^n} \omega^{n+1}, \tag{D20}$$

while in two dimensions

$$M(\omega) = \frac{1}{2\pi} \frac{\lambda\omega}{v_F c \sin(\arccos(c/v_F))} \approx \frac{1}{2\pi} \frac{\lambda \omega^n}{v_F c \omega_D^n}. \tag{D21}$$

We can also split the non-equilibrium Fermi distribution function into even and odd sectors:

$$f(x, k) = f_{even}(x, k) + f_{odd}(x, k), \tag{D22}$$

where $f_{even} = f_F(\epsilon, T_e(x))$, $f_{odd} = eEv_F \tau \partial_\epsilon f_F(\epsilon, T_e)$, and τ denotes the electron-impurity scattering time. After combining the even and odd sectors of the Boltzmann equations [8], we get the following coupled electron-boson diffusion equations:

$$D\partial_x^2 f(\epsilon, T_e) + I_{e-ph} = 0 \tag{D23}$$

$$\partial_x^2 n_B(\omega, T_b) = d(4\pi N_F \lambda / v_F \omega_D^n)^2 \omega^{2n} [n_B(\omega, T_b(x)) - n_B(\omega, T_e(x))]. \tag{D24}$$

Appendix E: Analytic expression of Θ_e in the drage regime

In the electron-boson drag regime, the bosons and electrons share the same temperatures: $\Theta_e = \Theta_b$. After combining with Eq.(15) and Eq.(16) in the main text,

$$\Theta_e = \Theta_b \tag{E1}$$

$$\Theta_e^2 + \frac{\gamma_e}{\gamma_b}\Theta_b^{d-n+1} = \frac{6}{\pi^2}\left[\frac{1}{8} - \frac{1}{2}\left(\frac{x}{L}\right)^2\right] \tag{E2}$$

one can solve Θ_e with different dimension d and scaling exponent n in Yukawa coupling as functions of $p = \gamma_b/\gamma_e$ and $\Theta_{0e}(x) = \sqrt{\frac{3}{4\pi^2}\left[1 - \left(\frac{2x}{L}\right)^2\right]}$:

- $d = 2, n = 1$:

$$\Theta_e(p, \Theta_{0e}) = \sqrt{\frac{p}{1+p}}\Theta_{0e} \tag{E3}$$

- $d = 3, n = 0$:

$$\Theta_e(p, \Theta_{0e}) = \frac{1}{\sqrt{2}}\sqrt{\sqrt{p^2 + 4p\Theta_{0e}^2} - p} \tag{E4}$$

- $d = 2, n = 0$ and $d = 3, n = 1$:

$$\Theta_e(p, \Theta_{0e}) = \frac{1}{3}\left(-p + \frac{2^{1/3}p^2}{\left(27\Theta_{0e}^2 p - 2p^3 + 3\sqrt{81\Theta_{0e}^4 p^2 - 12\Theta_{0e}^2 p^4}\right)^{1/3}} + \frac{\left(27\Theta_{0e}^2 p - 2p^3 + 3\sqrt{81\Theta_{0e}^4 p^2 - 12\Theta_{0e}^2 p^4}\right)^{1/3}}{2^{1/3}}\right) \tag{E5}$$